Coastal Engineering 55 (2008) 959–966

Contents lists available at ScienceDirect

Coastal Engineering

journal homepage: www.elsevier.com/locate/coastaleng

# Effects of wave age and air stability on whitecap coverage

Dag Myrhaug *, Lars Erik Holmedal

*Department of Marine Technology, Norwegian University of Science and Technology, NO-7491 Trondheim, Norway*

ARTICLE INFO

*Article history:*
Received 19 December 2007
Received in revised form 21 February 2008
Accepted 12 March 2008
Available online 28 April 2008

*Keywords:*
Whitecap coverage
Breaking waves
Wind generated waves
Wave age
Air stability
Air–sea interactions
Field data

ABSTRACT

The paper considers the effects of wave age and air stability on the whitecap coverage at sea. This is made by using the logarithmic mean wind velocity profile including a stability function as well as adopting a recent wave age dependent sea surface roughness formula. The results are valid for wind waves in local equilibrium with the steady wind. Examples of results demonstrate clear effects of wave age and air stability on the whitecap coverage. Comparisons are also made with field measurements by Sugihara et al. [Sugihara, Y., et al., 2007. Variation of whitecap coverage with wave-field conditions. J. Mar. Syst. 66, 47–60], representing unstable air stability conditions. Although the data basis is limited, the wave age independent Charnock sea roughness based predictions capture the main features of the observed whitecap coverage, suggesting a stronger dependence on air stability than on wave age in the data.



## 1. Introduction

Breaking of wind waves plays an important role in air–sea exchange processes due to the enhancement of turbulence and the entrainment of air. To quantify the occurrence of breaking wind waves is difficult; the whitecap coverage, which is defined as the area of whitecaps per unit sea surface, has often been used. Existing data on whitecaps show large scatter when they are plotted versus the wind speed only; other important factors are the stratification of the near-surface air boundary layer and the state of development of surface waves, see e.g. Sugihara et al. (2004, 2007). Massel (2007) gives a review of whitecap coverage at sea considering it from a wider perspective as wave breaking is one of the mechanisms which plays a major role in marine aerosol production. The boundary layer flow over the sea surface is also complicated by the sea surface roughness over waves, which depends on air–sea interactions; see e.g. Smith et al. (1996) and Jones and Toba (2001) for a further discussion.

For strong winds the effect of temperature stratification of the near-surface air boundary layer is minimal due to mixing of the air. However, for weaker and moderate winds, i.e. for wind velocities (at the 10 m elevation) up to about 25 m/s, the presence of stratification effects due to temperature gradients has been documented (Smith, 1980; Andersen and Løvseth, 1995). By analyzing wind speed observations over the Southern North Sea covering a period of about seven years, Coelingh et al. (1996) found that in spring the stratification is mainly stable, and in autumn it is mainly unstable, since the seawater temperature is lower (spring) and higher (autumn) than the air temperature. These results are summarized in Table 1 showing that stable and unstable conditions (caused by stratification) cover 85–90% of all hours in the various seasons of the year. Spillane et al. (1986) analyzed whitecaps observations (262 cases) with wind speed, water temperature and thermal stability. They documented that for wind speeds up to 18 m/s both stable, unstable and near-neutral conditions were present in the observations, thus justifying the relevance of the present study.

Sugihara et al. (2004) analyzed field observations of whitecap coverage and proposed the formula

$$W_c = \left[a(u_* - b)\right]^3 \; ; \; (a, b) = (2.20, 0.109) \tag{1}$$

where $W_c$ is the whitecap coverage given in percent, $u_*$ (m/s) is the friction velocity equal to the square root of the vertical flux of horizontal momentum at the sea surface. The basis for Sugihara et al. to use Eq. (1), was the results by Phillips (1985) who found the dissipation rate of wave energy to be proportional to $u_*^3$ based on the equilibrium spectrum of wind waves. Moreover, there is a connection between the dissipation rate and the wave breaking; Sugihara et al. (2004) assumed a linear relationship between $W_c$ and the dissipation rate and found support for this assumption in the data, and the consequence is Eq. (1). Sugihara et al. (2004) plotted $W_c^{1/3}$ versus $u_*$ and $W_c^{1/3}$ versus the mean wind speed at the 10 m elevation, $U_{10}$. The dependence of $W_c^{1/3}$ on $u_*$ supported the validity of Eq. (1), but the

* Corresponding author.
*E-mail address:* dag.myrhaug@ntnu.no (D. Myrhaug).

0378-3839/$ – see front matter © 2008 Elsevier B.V. All rights reserved.
doi:10.1016/j.coastaleng.2008.03.005

**Table 1**
Percentage of atmospheric stability versus season of the year

| Condition | Season | | | | |
|---|---|---|---|---|---|
| | Spring | Summer | Fall | Winter | Annual |
| Stable | 40–50 | 30–40 | 10–25 | 20–30 | 30–35 |
| Unstable | 40–45 | 55–60 | 65–80 | 60–75 | 55–60 |
| Neutral | 10–15 | ~10 | ~10 | 10–15 | ~10 |

data scatter was larger than for $W_c^{1/3}$ versus $U_{10}$. This was attributed to the larger uncertainties in estimating $u_*$ than measuring $U_{10}$. Their data covered both near-neutral and unstable stratification, and they found that air instability promotes wave breaking. They also distinguished between the state of development of the waves; whether the sea surface was in the state of developing waves or decaying waves. This was classified on the basis of time series of the significant wave height $H_s$; developing waves if $H_s$ increased with time and decaying waves if $H_s$ decreased with time. For a given value of $U_{10}$ they found that the whitecap coverage was larger for decaying than for developing waves. Moreover, from directional wave spectra they divided their data into groups of pure windsea, swell-dominated sea as well as combined sea, finding that whitecaps are mainly produced by wind waves and suppressed by the presence of swell. More details are given in Sugihara et al. (2004).

Recently Sugihara et al. (2007) followed up the analysis presented in Sugihara et al. (2004) by also including a second data set collected during another period at the same location. By introducing the second data set the fit of Eq. (1) to data gave slightly different coefficients, i.e. $(a, b)$= (2.12, 0.074). However, by considering the scatter in the data, the different values of $a$ and $b$ are not significant; therefore Eq. (1) is used with the original values of $a$ and $b$ to serve the purpose of demonstrating the qualitative effects of wave age and air stability on whitecaps. Sugihara et al. (2007) also extended the analysis by including the wave age; they found that the whitecap coverage increases with the wave age for the same wind speed conditions. Further details are given in Sugihara et al. (2007). Lafon et al. (2007) also analyzed field observations and studied the whitecap coverage for steady and unsteady wave field conditions in the coastal zone of the Mediterranean Sea. They proposed a wave age dependent model for the whitecap coverage with a peak of the whitecap coverage for intermediate wave ages; the formula reflects the characteristics of the different sea state conditions taking into account the influence of both wind and waves.

Another quantity of interest is the breaking frequency $f_{br}$. Phillips (1985) used the whitecap residence time to determine $f_{br}$. By assuming the residence time to be constant and denoting it as $t_{disrupt}$ (as the whitecaps is understood as disruption of the surface), the breaking frequency is given as (Eifler, 2005)

$$f_{br} = \frac{W_c}{t_{disrupt}} \;;\; t_{disrupt} = 0.5\text{s} \tag{2}$$

This value of $t_{disrupt}$ is based on Snyder et al.'s (1983) results from open-ocean measurements, although other investigations have indicated somewhat lower values (~0.3 s). More details, as well as a review of the topic, are given in Eifler (2005).

The purpose of the present paper is to investigate the effects of wave age and air stability on the whitecap coverage at sea. This is achieved by using Eq. (1) and to determine $u_*$ by using the logarithmic mean wind velocity profile including a stability function according to Kraus and Businger (1994) accounting for the air stability, as well as adopting a recent sea surface roughness formulation including the wave age according to Volkov (2001). The wave age independent Charnock (1955) roughness formula is also used as a reference. The results are valid for the development of wind waves which are in local equilibrium with the wind, and for a given steady wind speed that starts to blow over flat water without waves until the waves are fully developed. Thus, the approach does not cover situations with unsteady wind, or for wind over the sea surface in sea states of developing or decaying waves as defined by Sugihara et al. (2004). Comparisons are also made with field measurements by Sugihara et al. (2007) which fulfil these conditions, representing unstable air stability. Although the data basis is limited, the wave age independent Charnock sea roughness based predictions capture the main features of the observed whitecap coverage, suggesting a stronger dependence on air stability than on wave age in the data.

## 2. Theoretical background

### 2.1. Sea surface shear stress

The effect of air stability on the sea surface boundary layer structure usually scales with the dimensionless stability parameter $\zeta=z/L$. Here $z$ is the height above the sea surface and $L$ is the buoyancy length scale known as the Monin–Obukhov length defined as $L=-u_*^3 T_0/g\kappa Q_0$ (Arya, 1982); $\kappa$ is the von Karman's constant (=0.4), $T_0$ is the sea surface temperature, $Q_0$ is the sea surface kinematic heat flux taken as positive upwards from the sea surface, which can be parameterized as $Q_0=-C_T U_{10}(T_{10}-T_0)$ where $C_T$ is the sea surface temperature coefficient, and $T_{10}$ is the air temperature at the 10 m elevation. Physically $\zeta$ expresses the ratio between the potential energy required at a particular level to mix the density gradient (caused by the potential temperature gradient) and the turbulent kinetic energy supplied by the wind shear at the level. For $\zeta<0$, $\zeta=0$, $\zeta>0$ the stratification is referred to as unstable, neutral and stable, respectively. For large values of $|L|$, turbulent mixing dominates buoyancy in the boundary layer. In general $|\zeta|\ll 1$ close to the surface, regardless of the magnitude of $|L|$.

Close to the surface Kraus and Businger (1994) give the mean wind velocity profile

$$U(z) = \frac{u_*}{\kappa}\left[\ln\frac{z}{z_0} - \psi(\zeta)\right] \tag{3}$$

where $\psi(\zeta)$ is often referred to as the stability function taking into account stratification effects, and $z_0$ is the sea surface roughness which generally depends on $u_*$ and will be discussed later. Following Kraus and Businger (1994), the stability function is parameterized as

$$\psi = \ln\frac{(1+x^2)(1+x)^2}{8} - 2\ \text{arc tg}\, x + \frac{\pi}{2},\ x = (1-16\zeta)^{1/4};\ \text{unstable}(\zeta<0) \tag{4}$$

$$\psi = -5\zeta;\ \text{stable}(\zeta>0) \tag{5}$$

One should note that Eqs. (4) and (5) are derived from observations over land, but a number of indirect results suggest that these equations are also valid over water (Kraus and Businger, 1994). According to Panofsky and Dutton (1984), Eq. (4) is the most widely used parameterization for unstable air, although other parameterizations exist. For stable air all measurements suggest Eq. (5), with estimates of the constant in the range 4.7–5.2 (instead of using 5); more details are given in Panofsky and Dutton (1984). However, one should note that a recent analysis of Norwegian coastal wind measurements gave slightly different values of the stability function (Heggem, 1997); i.e. Eq. (4) with $x=(1-17\zeta)^{1/4}$ and $\psi=-3.6\zeta$ for unstable and stable conditions, respectively, while the Charnock constant was found to be 0.0172 (see the next section). The shape of the atmospheric boundary layer by using Eqs. (3)–(5) for different values of $L$ is shown in e.g. Young (1998, Fig. 1).

For $z=z_{10}=10$ m, Eq. (3) can be rearranged to

$$u_* = \frac{\kappa U_{10}}{\ln\frac{z_{10}}{z_0} - \psi\left(\frac{z_{10}}{L}\right)} \tag{6}$$

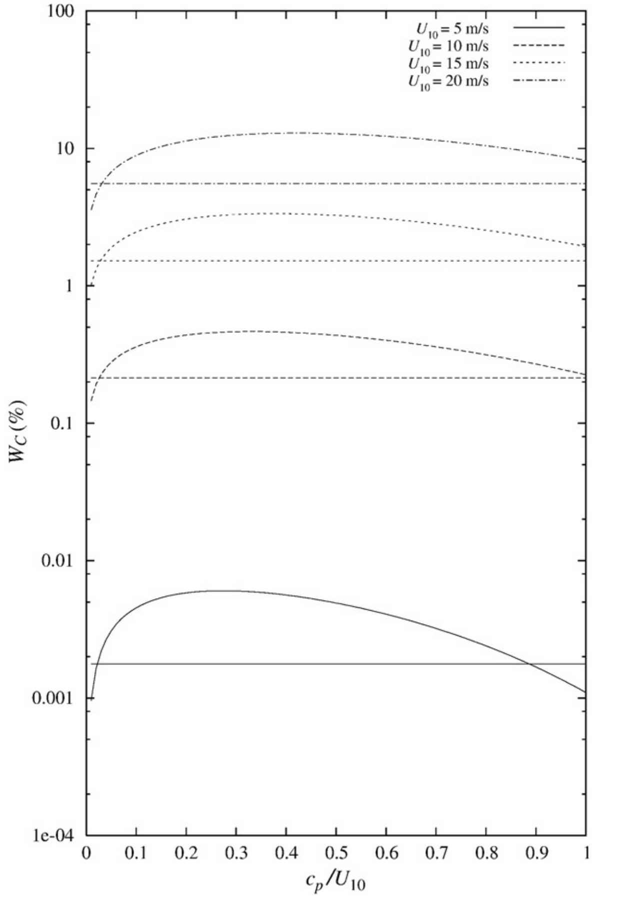


**Fig. 1.** Whitecap coverage $W_c$ for neutral stability versus wave age $c_p/U_{10}$ for $U_{10}$=5, 10, 15, 20 m/s for Volkov (curved lines) and Charnock (horizontal lines).

where $z_0$ depends on $u_*$. Now $u_*$ can be determined from Eq. (6) by iteration for given values of $U_{10}$ and $L$ by substituting an appropriate model of $z_0$ (see below), and the sea surface drag coefficient can be expressed as

$$C_D = \left(\frac{u_*}{U_{10}}\right)^2 \tag{7}$$

The sea surface drag coefficient for neutral stability, $C_{Dn}$, is then given from Eqs. (6) and (7) as

$$C_{Dn} = \kappa^2 \left(\ln \frac{z_{10}}{z_0}\right)^{-2} \tag{8}$$

### 2.2. Sea surface roughness parameter

The roughness of the sea surface depends on air–sea interaction conditions and is difficult to estimate; no consistent theory exists on the relation between $z_0$ and the roughness of the sea surface. Since Charnock (1955) proposed his well-known formula from a dimensional argument, many different formulas have been proposed, see e.g. Smith et al. (1996). Essentially it is a discussion of to what extent laboratory and ocean-wave systems actually involve precisely the same physics, i.e. if extrapolation of the laboratory data to the field using non-dimensional quantities such as wave age or dimensionless fetch is feasible. Hopefully, fundamental studies in the laboratory (see e.g. Banner and Peirson, 1998) together with field investigations will contribute to clarify the matter.

Volkov (2001) provided the following expression for the sea surface roughness:

$$z_0^* = 0.03x \exp(-0.14x) \text{ for } 0.35 < x < 35, \; z_0^* = 0.008 \text{ for } 35 \le x \tag{9}$$

where $z_0^* = gz_0/u_*^2$ is the dimensionless roughness, $x = c_p/u_*$ is the wave age, and $c_p$ is the phase speed associated with wind waves with spectral peak frequency $\sigma_p$. Eq. (9) is obtained as a fit to existing data (see Fig. 10.6, Volkov, 2001). The non-dimensional roughness has a maximum value at $c_p/u_*$ around 10 (see Fig. 1.15, Jones et al., 2001), and for $c_p/u_* > 35$ (which can also represent light wind over swell) the non-dimensional roughness is near 0.01. Volkov's formula is based on the state of knowledge at that time. It should be noted that Eq. (9) is valid for steady wind and wind waves in local equilibrium with the wind in a laterally homogeneous flow; further background and details are given in Volkov (2001) and Jones et al. (2001). Moreover, the influence of unsteady wind speed on the wave response is discussed in e.g. Toba and Jones (2001).

Here the Volkov (2001) model will be used to serve the purpose of taking into account the effect of wave age, and the wave age independent Charnock (1955) formula will be used as a reference; the latter formula is given by

$$z_0^* = \beta\,; \; \beta = 0.0185 \tag{10}$$

where the given $\beta$-value is the Charnock constant. It should be noted that this $\beta$-value is not considered conclusive as the values of $\beta$ are given within a range of 0.015 to 0.025 (Toba et al., 1990). By using the dispersion relationship for linear waves in deep water, the phase speed associated with waves with spectral peak period

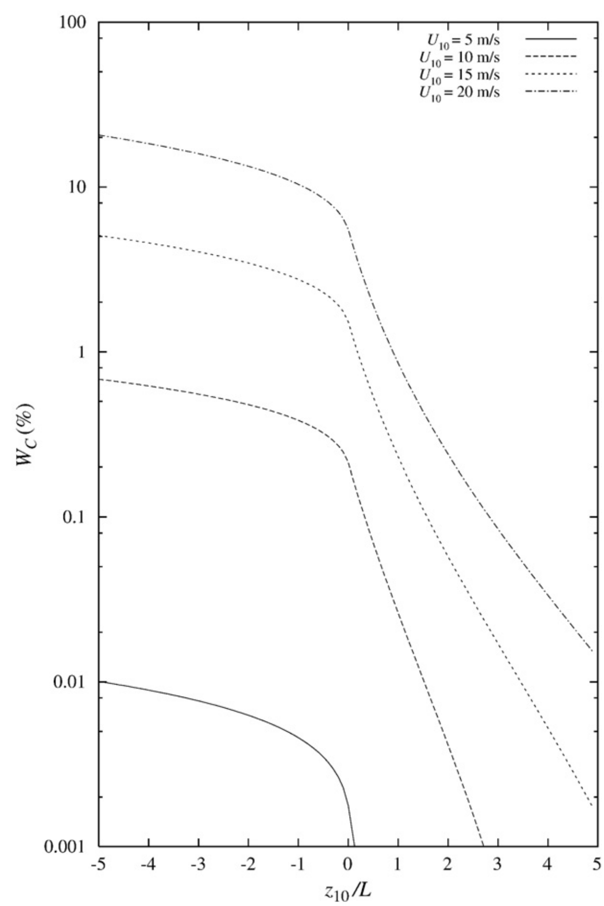


**Fig. 2.** Whitecap coverage $W_c$ versus air stability $z_{10}/L$ for $U_{10}$=5, 10, 15, 20 m/s for Charnock.

$T_p = 2\pi/\sigma_p$ is given by $c_p = gT_p/2\pi$, and thus the wave age can be expressed as $(g/2\pi)(T_p/u_*)$. An alternative expression for the wave age is $c_p/U_{10}$; found by replacing $u_*$ by $U_{10}$. Realistic wave age limits representing wind waves are often taken as $0.03 \le c_p/U_{10} \le 1.0$ (Toba et al., 1990).

## 3. Results and discussion

The effects of wave age and air stability on the whitecap coverage are exemplified for weak to moderate wind speeds, covering realistic conditions at sea valid for wind waves in local equilibrium with the steady wind. Comparisons with field observations of whitecap coverage for pure windsea conditions given by Sugihara et al. (2007) are also presented.

### 3.1. Parameter study of whitecap coverage

Fig. 1 shows $W_c$ for neutral stability versus the wave age $c_p/U_{10} = gT_p/2\pi U_{10}$ in the range 0.03 to 1.0 for $U_{10}$ = 5, 10, 15 and 20 m/s according to the wave age dependent Volkov model of $z_0$ and for the wave age independent Charnock model of $z_0$. First, it is noted that $W_c$ increases as $U_{10}$ increases for a given wave age; the increase is significant, covering a range of four decades from $10^{-3}$ to 10 for these values of $U_{10}$. Moreover, for a given value of $U_{10}$ it appears that $W_c$ increases as the wave age increases for young waves; then $W_c$ reaches a maximum at a wave age in the intermediate range 0.25 to 0.4 depending on $U_{10}$, before $W_c$ decreases and approaches values close to the Charnock results for fully developed waves.

As a reference case $W_c$ versus the air stability $z_{10}/L$ for $U_{10}$ = 5, 10, 15 and 20 m/s using the wave age independent Charnock roughness is shown in Fig. 2. For a given wind speed $U_{10}$ it appears that: $W_c$ decreases as the air stability $z_{10}/L$ increases, because air stability suppresses wave breaking. Furthermore, $W_c$ increases as the flow becomes more unstable, i.e. as $|z_{10}/L|$ increases for $z_{10}/L < 0$, because air instability enhances wave breaking. The latter is consistent with the results of field data analysis conducted by Sugihara et al. (2004).

Fig. 3 *a* to *d* shows contour plots of $W_c$ versus the air stability $z_{10}/L$ and the wave age $c_p/U_{10}$ for $U_{10}$ = 5, 10, 15 and 20 m/s by using the wave age dependent Volkov roughness. First, the strong effect of $U_{10}$

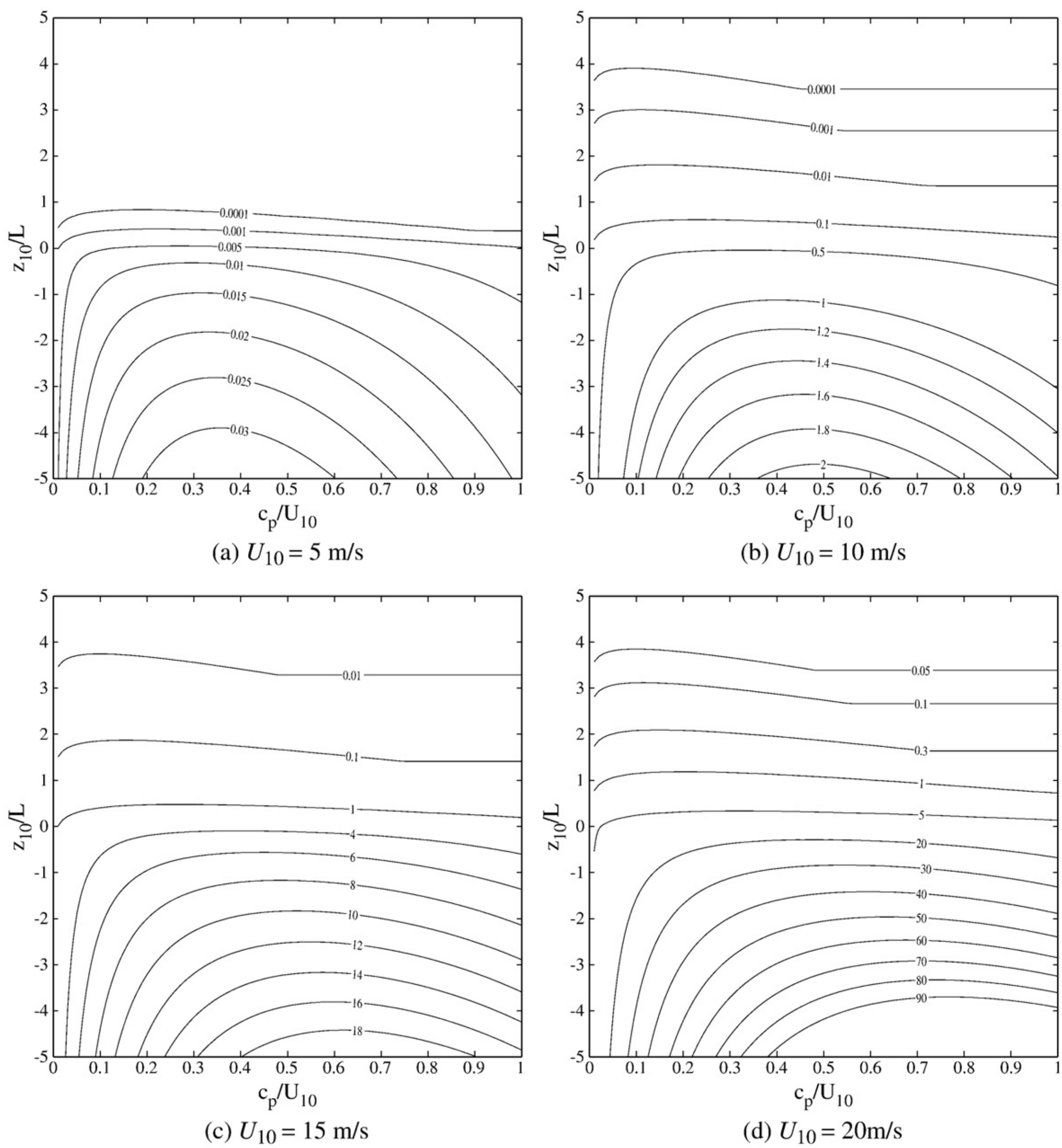


**Fig. 3.** Contour plots of whitecap coverage $W_c$ versus air stability $z_{10}/L$ and wave age $c_p/U_{10}$ for (a) $U_{10}$ = 5 m/s; (b) $U_{10}$ = 10 m/s; (c) $U_{10}$ = 15 m/s; (d) $U_{10}$ = 20 m/s.

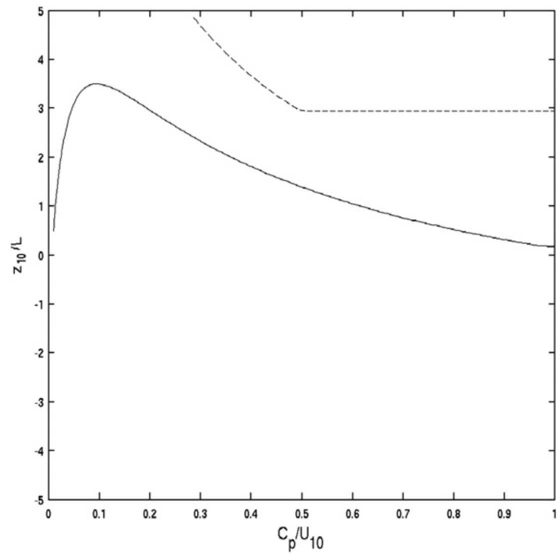


**Fig. 4.** Contour plots of $Re=u_*z_0/\nu=0.17$ versus air stability $z_{10}/L$ and wave age $c_p/U_{10}$ for $U_{10}=5$ m/s (lower full curve) and $U_{10}=10$ m/s (upper broken curve); note that the flow is smooth turbulent within the regions above these curves, respectively, and that $\nu=1.4\cdot10^{-5}$ m$^2$/s is used.

on $W_c$ for a given wave age and air stability is noted; similar to that observed in Fig. 1. Second, for a given wave age and wind speed, the dependence on air stability is qualitatively the same as those by using the wave age independent Charnock results in Fig. 2. That is, air stability and air instability suppresses and enhances wave breaking as compared with neutral flow, respectively. Third, for a given $U_{10}$ and air stability for unstable conditions ($z_{10}/L<0$), $W_c$ increases as $c_p/U_{10}$ increases for lower to moderate wave ages, while $W_c$ decreases as $c_p/U_{10}$ increases towards fully developed waves. This behaviour agrees qualitatively with that observed for neutral flow based on the Volkov results in Fig. 1. Moreover, for given $U_{10}$ and air stability for stable conditions ($z_{10}/L>0$), the effect of wave age on $W_c$ is small, see e.g. the results for $U_{10}=20$ m/s (Fig. 3d). Overall, Fig. 3 shows that the $W_c$-dependence on the air stability is generally an order of magnitude larger than the dependence on the wave age. This is particularly evident for stable conditions ($z_{10}/L>0$) in Fig. 3, where the results only vary slightly with wave age.

Fig. 4 shows contour plots of the critical Reynolds number, $Re=0.17$, versus $z_{10}/L$ and $c_p/U_{10}$ for $U_{10}=5$ and 10 m/s. Here $Re=u_*z_0/\nu$, where $\nu$ is the kinematic viscosity of the air. Eq. (3) is strictly only valid for rough turbulent flow ($Re>2.3$), but it might also be used in the transitional smooth to rough turbulent flow regime ($0.17<Re<2.3$) (Schlichting, 1979). This means that the flow is smooth turbulent within the regions above the curves in Fig. 4. Thus the results in Fig. 3a (for $U_{10}=5$ m/s) are valid in the region below the full curve in Fig. 4. Similarly, the results in Fig. 3b (for $U_{10}=10$ m/s) are valid in the region below the broken curve in Fig. 4. However, the results for $U_{10}=15$ (Fig. 3c) and 20 m/s (Fig. 3d) are not affected by these restrictions for the given parameter range of $z_{10}/L$ and $c_p/U_{10}$, since the flow is rough turbulent (or smooth to rough turbulent) in the whole region.

### *3.2. Comparison with field measurements*

Here comparisons are made with the Sugihara et al. (2007) data referred to in Section 1. The data used here represent the "pure windsea" conditions given in Table 1 of their paper, representing 24 time series; 11 time series from observation *A* and 13 time series from observation *B*; all represent unstable conditions and contain wave age effects. These data satisfy the steady wind conditions as described in Section 2.2. By using the results in Section 2.1, the Monin–Obukhov length $L$ can be evaluated as $L=u_*^3T_0/g\kappa C_T U_{10}(T_{10}-T_0)$. The values of $U_{10}$, $\Delta T=T_{10}-T_0$, $u_*$, $T_p$ and $W_c$ are given in Sugihara et al. (2007, Table 1), while $T_0$ is not specified. Thus the stability parameter takes the form

$$\frac{z_{10}}{L}=\frac{z_{10}g\kappa C_T U_{10}\Delta T}{u_*^3 T_0} \tag{11}$$

Here the sea surface temperature $T_0=5$ °C is chosen, and the sea surface temperature coefficient is taken as $C_T=0.0012$ (Kraus and Businger, 1994).

Now the predicted results are obtained by using Eq. (11) for $z_{10}/L$ in Eq. (6) together with Eq. (9) (Volkov) or Eq. (10) (Charnock) for $z_0$, as well as Eqs. (4) and (5) for the stability function. This means that $z_{10}/L$ is part of the iteration scheme determining $u_*$, which is different from the calculation in Section 3.1, where $z_{10}/L$ was taken as a given (independent) variable.

Fig. 5 shows the predicted versus the measured values of $u_*$, and it appears that the predictions based on the Charnock roughness agree slightly better with the data than the predictions based on the Volkov roughness. Except for the two data points of $u_*$ with values close to 0.8 representing the Volkov based predictions, the predicted to measured ratios for both Charnock and Volkov are within a range of approximately 0.75 to 1.6.

Fig. 6 shows the predicted versus the measured values of $W_c$, and it appears that the wave age independent Charnock based predictions (Fig. 6a) agree better with the measurements than the wave age dependent Volkov based predictions (Fig. 6b), which is consistent with the results in Fig. 5. Here, and in the remaining figures, the data are divided into the following three groups based on the wind speed $U_{10}$; 4–7 m/s, 7–10 m/s and 10–13 m/s. Fig. 6 shows that the whitecap coverage increases with wind speed, as expected. The fact that $W_c$ is best predicted by using the Charnock formula suggests that the $W_c$-dependence on wave age is small. This will be discussed further in the following.

Fig. 7 shows $W_c$ versus wave age; the measurements (Fig. 7a), and the Charnock (Fig. 7b) and the Volkov (Fig. 7c) based predictions. The measurements (Fig. 7a) do not reveal any clear dependence of $W_c$ on wave age for given values of $U_{10}$, although the data for 7 m/s$<U_{10}<$10 m/s show a weak tendency of $W_c$ to increase with increasing wave age. Sugihara et al. (2007) analysed these pure windsea data in a slightly different way by using the wave age $x=c_p/u_*$ defined in Section 2.2. They divided the data into two groups based on this wave age and found that $W_c$ increases with wave age for a given wind speed,

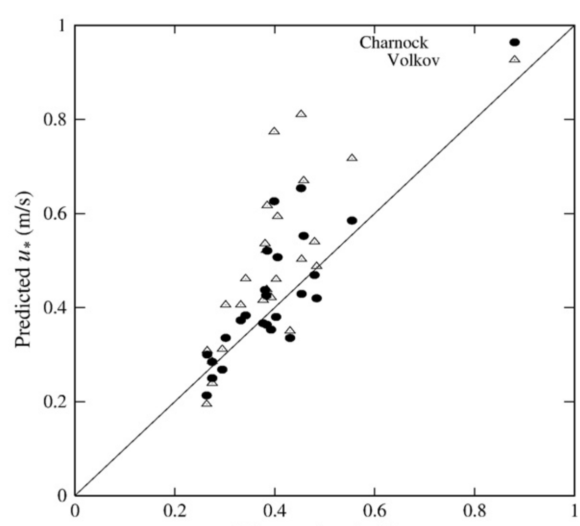


**Fig. 5.** Predicted versus measured values of the friction velocity $u_*$; the predictions are based on the Charnock and Volkov roughnesses; the measurements represent pure windsea from Sugihara et al. (2007, Table 1).

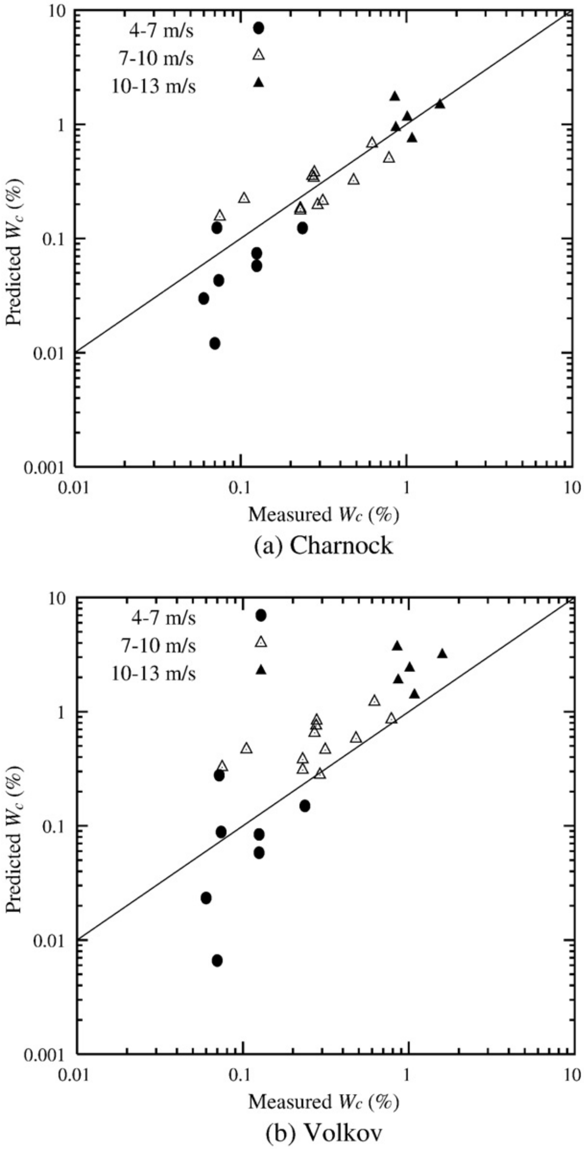


**Fig. 6.** Predicted versus measured values of whitecap coverage $W_c$ for three groups of the wind speed $U_{10}$; 4–7 m/s, 7–10 m/s, 10–13 m/s. The measurements represent pure windsea from Sugihara et al. (2007). Predictions based on: (a) Charnock roughness; (b) Volkov roughness.

which is consistent with the observation for 7 m/s$<U_{10}<$10 m/s. It is also noted that the wave age independent Charnock based predictions (Fig. 7b) are qualitatively similar to the wave age dependent Volkov based predictions (Fig. 7c), which supports the interpretation of the results in Fig. 6 that the $W_c$-dependence on wave age is small.

Fig. 8 shows $W_c$ versus air stability represented by $\Delta T$; the measurements (Fig. 8a), and the Charnock (Fig. 8b) and the Volkov (Fig. 8c) based predictions. Although the data are scattered, they show a weak tendency of $W_c$ to increase as $|\Delta T|$ increases; i.e. as the air instability increases, for given values of $U_{10}$. This trend is clearest observed in the measurements (Fig. 8a). These features are consistent with the predictions shown in Fig. 2, in the sense that the Charnock based predictions for unstable conditions ($z_{10}/L<0$), show an increase of $W_c$ as $|z_{10}/L|$ increases for given values of $U_{10}$. It is also noted that the Charnock based predictions of the field data (Fig. 8b) are qualitatively similar to the corresponding Volkov based predictions (Fig. 8c), which supports the previous results of weak $W_c$-dependence on wave age, and a stronger dependence on air stability. Moreover, the Charnock (Fig. 8b) and Volkov (Fig. 8c) based predictions show a tendency of $W_c$ to increase as $|\Delta T|$ increases for 7 m/s$<U_{10}<$10 m/s. Sugihara et al. (2004) analysed their data from observation $A$ in a slightly different way by dividing the data into two groups based on $\Delta T$, and found that $W_c$ increases with increasing air instability for a given wind speed, which is overall consistent with the observations in Fig. 8.

Overall, the stronger $W_c$-dependence on air stability than on wave age for given values of $U_{10}$ as suggested by the results in Figs. 6–8, is consistent with the theoretical predictions in Section 3.1; see the discussion of the results in Fig. 3.

Fig. 9 shows the predicted versus the measured values of $z_{10}/L$ given in Eq. (11), i.e. based on the calculated and observed values of $u_*$,

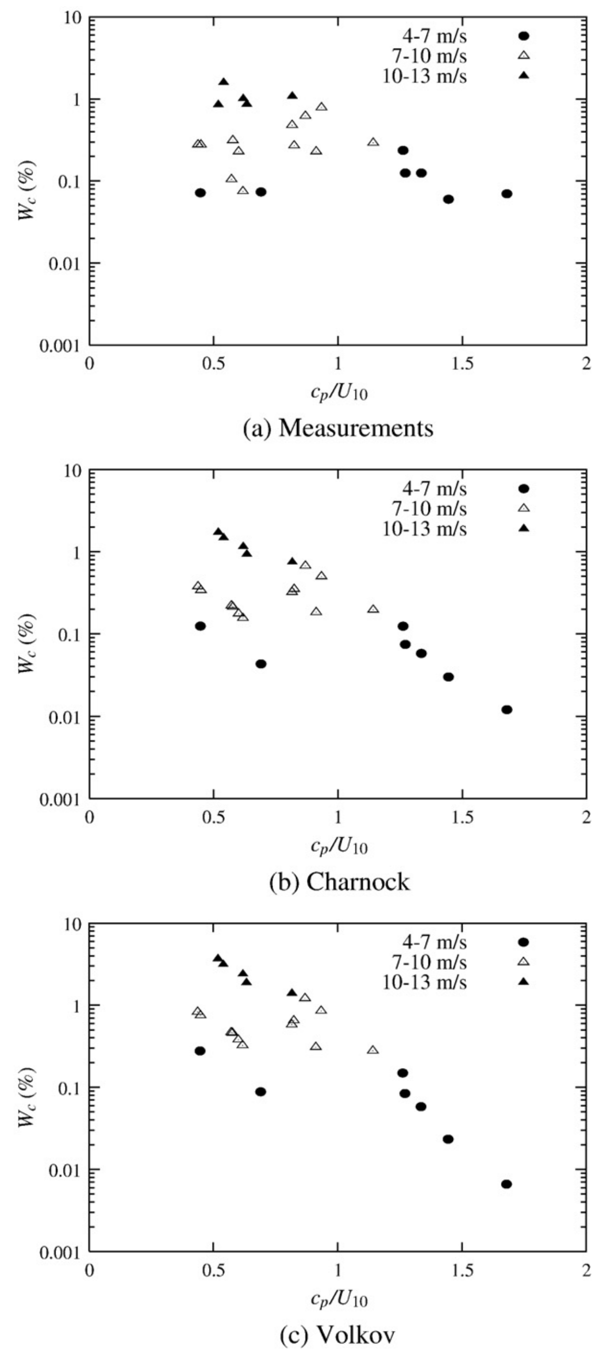


**Fig. 7.** Whitecap coverage $W_c$ versus wave age $c_p/U_{10}$ for the three groups of $U_{10}$ as in Fig. 6: (a) measurements representing pure windsea from Sugihara et al. (2007); (b) Charnock based predictions; (c) Volkov based predictions.

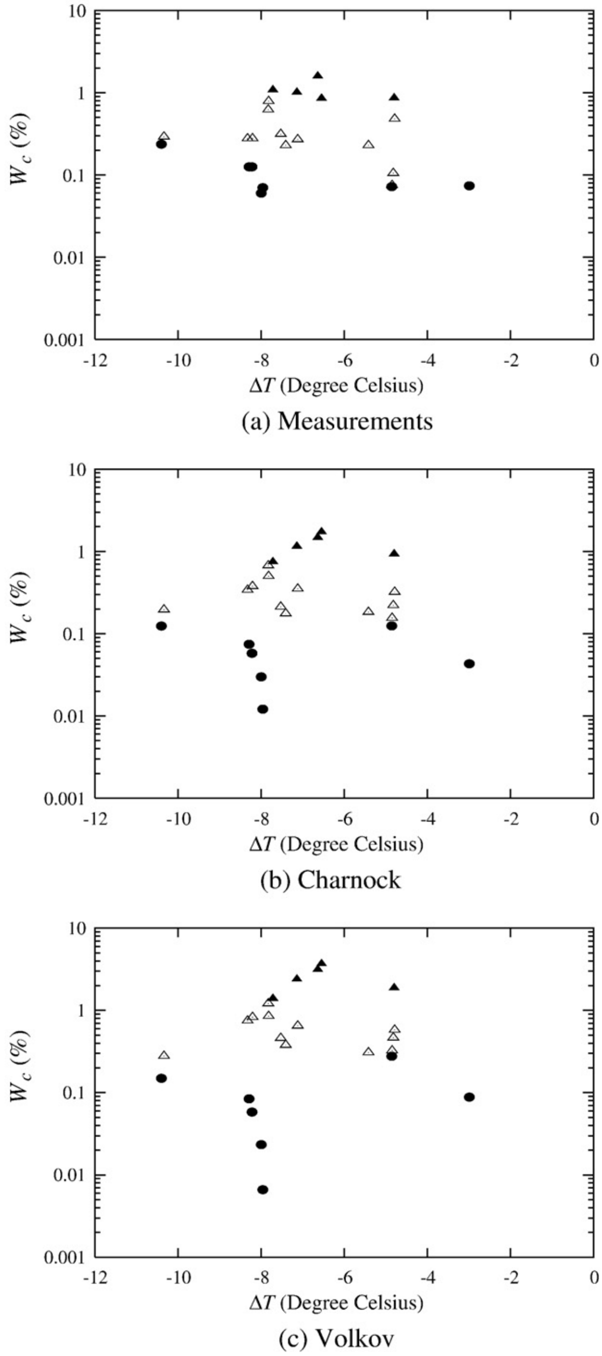


**Fig. 8.** Whitecap coverage $W_c$ versus air stability represented by $\Delta T$ for the three groups of $U_{10}$ (the symbols have the same meaning as in Fig. 7): (a) measurements representing pure windsea from Sugihara et al. (2007); (b) Charnock based predictions; (c) Volkov based predictions.

respectively. A significant scatter is observed; for the Charnock based predictions (Fig. 9a) the predicted to measured ratio is in the range 0.25 to 2, while it is in the range 0.1 to 2.5 for the Volkov based predictions (Fig. 9b).

Finally, it should be noted that the flow is in the rough turbulent regime. By using the Charnock roughness in Eq. (10) and $\nu=1.4\cdot10^{-5}$ m$^2$/s, the Reynolds number, $Re=u_*z_0/\nu$, is found to be larger than 2.5 for the observed data, i.e. the flow is rough turbulent.

Although the data basis used for comparison is limited, it appears that the main features of the observed whitecap coverage are best captured by the wave age independent Charnock based predictions.

## 4. Summary

For wind waves which are in local equilibrium with the wind, examples of results covering a wide parameter range typical for field conditions have demonstrated:

1. Clear effects of wave age and air stability on the whitecap coverage.
2. For a given air stability, the whitecap coverage reaches a maximum for intermediate wave age.
3. The whitecap coverage dependence on air stability is generally an order of magnitude larger than the dependence on wave age.
4. Air stability and air instability suppresses and enhances wave breaking as compared to neutral flow, respectively; the latter agrees qualitatively with the results in Sugihara et al. (2004).

Predicted whitecap coverage has been compared with field measurements by Sugihara et al. (2007) representing unstable air stability over pure windsea. Although the data basis is limited, it appears that the main features of the observed whitecap coverage are best captured by the wave age independent Charnock based predictions, suggesting a stronger dependence on air stability than on wave age in the data.

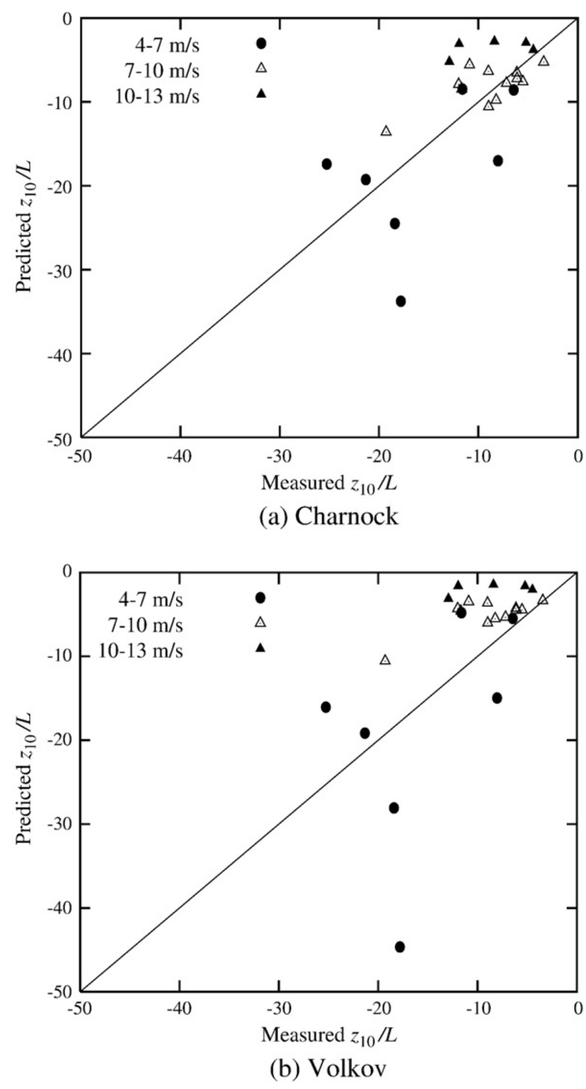


**Fig. 9.** Predicted versus measured values of air stability $z_{10}/L$ for the three groups of $U_{10}$ as in Fig. 6: predictions based on (a) Charnock roughness; (b) Volkov roughness; the measurements represent pure windsea from Sugihara et al. (2007).

## References

Andersen, O.J., Løvseth, J., 1995. Gale force maritime wind. The Frøya data base. Part 1: Sites and instrumentation. Review of the data base. J. Wind Eng. Ind. Aerodyn. 57, 97–109.
Arya, S.P., 1982. Atmospheric boundary layers over homogeneous terrain. In: Plate, E. (Ed.), Engineering Meteorology. Elsevier, New York, pp. 233–267.
Banner, M.L., Peirson, W.L., 1998. Tangential stress beneath wind-driven air–water interface. J. Fluid Mech. 364, 115–145.
Charnock, H., 1955. Wind stress on a water surface. Q. J. R. Meteorol. Soc. 81, 639–640.
Coelingh, J.P., et al., 1996. Analysis of wind speed observations over the North Sea. J. Wind Eng. Ind. Aerodyn. 61, 51–69.
Eifler, W., 2005. The near-surface boundary layer. In: Baumert, H.Z., et al. (Ed.), Marine Turbulence. Cambridge University Press, Cambridge, UK, pp. 250–272.
Heggem, T. 1997. Measurements of coastal wind and temperature. Sensor evaluation, data quality and wind structures, Dr.Sci. thesis, Dept. of Physics, NTNU, Trondheim, Norway.
Jones, I.S.F., Toba, Y., 2001. Wind Stress over the Ocean. Cambridge University Press, Cambridge, UK.
Jones, I.S.F., et al., 2001. Overview. In: Jones, I.S.F., Toba, Y. (Eds.), Wind Stress over the Ocean. Cambridge University Press, Cambridge, UK, pp. 1–33.
Kraus, E.B., Businger, J.A., 1994. Atmosphere-Ocean Interaction. Oxford University Press, New York.
Lafon, C., et al., 2007. Whitecap coverage in coastal environment for steady and unsteady wave field conditions. J. Mar. Syst. 66, 38–46.
Massel, S.R., 2007. Ocean Waves Breaking and Marine Aerosol Fluxes. Springer, New York.
Panofsky, H.A., Dutton, J.A., 1984. Atmospheric Turbulence. John Wiley & Sons.
Phillips, O.M., 1985. Spectral and statistical properties of the equilibrium range in wind-generated gravity waves. J. Fluid Mech. 156, 505–531.
Schlichting, H., 1979. Boundary Layer Theory, 7th edition. McGraw-Hill, New York.
Smith, S.D., 1980. Wind stress and heat flux over the ocean in gale force winds. J. Phys. Oceanogr. 10, 709–726.
Smith, S.D., et al., 1996. Air–sea fluxes: 25 years of progress. Bound.-Layer Meteorol. 78, 247–290.
Snyder, R.L., et al., 1983. On the formation of whitecaps by a threshold mechanism, Part III: field experiments and comparison with theory. J. Phys. Oceanogr. 13, 1505–1518.
Spillane, M.C., et al., 1986. Whitecaps and global fluxes. In: Monahan, E.C., MacNiocaill, G. (Eds.), Oceanic Whitecaps. D. Reidel Publ. Company, Dordrecht, The Netherlands, pp. 209–218.
Sugihara, Y., et al., 2004. Imaging measurement of whitecaps at sea observation tower. Proc. 29th Conf. on Coastal Eng., vol. 1. ASCE, Lisbon, Portugal, pp. 1082–1092.
Sugihara, Y., et al., 2007. Variation of whitecap coverage with wave-field conditions. J. Mar. Syst. 66, 47–60.
Toba, Y., et al., 1990. Wave dependence on sea-surface wind stress. J. Phys. Oceanogr. 20, 705–721.
Toba, Y., Jones, I.S.F., 2001. The influence of unsteadiness. In: Jones, I.S.F., Toba, Y. (Eds.), Wind Stress over the Ocean. Cambridge University Press, Cambridge, UK, pp. 190–205.
Volkov, Y., 2001. The dependence on wave age. In: Jones, I.S.F., Toba, Y. (Eds.), Wind Stress over the Ocean. Cambridge University Press, Cambridge, UK, pp. 206–217.
Young, I.R., 1998. An experimental investigation of the role of atmospheric stability in wind wave growth. Coast. Eng. 34, 23–33.